

## Formation and Technology of SiOF Films as Intermetal Dielectric by Helicon Wave Plasma CVD

Chi Kyu Choi

*Department of Physics, Cheju National University, Cheju 690-756, Korea*

Kwang Man Lee

*Department of Electronic Engineering, Cheju National University, Cheju 690-756, Korea*

Duk-soo Kim

*Department of Chemistry, Cheju National University, Cheju 690-756, Korea*

Hong-Young Chang

*Department of Physics, Korea Advanced Institute of Science and Technology, Taejon 305-701, Korea*

### Abstract

The deposited SiOF films by a helicon wave plasma CVD method have been characterized using Fourier transform infrared spectroscopy and ellipsometry. High density plasma of  $>10^{12} \text{ cm}^{-3}$  can be obtained on a substrate at low pressure ( $<10 \text{ mTorr}$ ), rf power of  $>400 \text{ W}$  and magnetic field strength of 707 Gauss. A gas mixture of  $\text{SiF}_4$ ,  $\text{O}_2$ , and Ar was used to deposit SiOF films on 5-inch Si(100) wafers not intentionally heated. Optical emission spectroscopy was used to study the relation between the relative densities of the radicals and the deposition mechanism. Discharge conditions such as gas composition, sheath potential, and the relative densities of the radicals affect the properties of the film. The dependence of refractive index on  $\text{SiF}_4/\text{O}_2$  flow rate ratio decreases from 1.37 to 1.08 as flow rate ratio increases from 0.2 to 1.0. This value is lower than that of thermal oxide and depends on F concentration. The relative dielectric constant, leakage current and dielectric breakdown are about 3.0,  $<10^{-9} \text{ A/cm}^2$  and  $>12 \text{ MV/cm}$ , respectively. It shows that the formed SiOF films by helicon wave plasma CVD have capability for interlayer formation in future ULSI multilevel interconnections.

## I. INTRODUCTION

Miniaturization of electronic circuits with increased complexity and multilevel metal layers demand new intermetal dielectric (IMD) materials with low dielectric constants. Present aluminum interconnects with silicon dioxide as IMD layers will result in high parasitic capacitance and crosstalk interference in high density devices<sup>(1,2)</sup>. As the operating speeds reach the gigahertz regime and the density of the device increases, the rate of signal transmission within the device is limited by the capacitance between the lines and is related to the delay constant. The most desired IMD material that can be used in advanced high density semiconductor devices should have a low dielectric constant, low mechanical stress, high thermal stability (>450 °C) and low moisture absorption<sup>(3)</sup>. One of the most promising IMD materials that provides a modest reduction in the dielectric constant but retains many of the properties of silicon dioxide is fluorinated silicon dioxide.  $F_xSiO_y$  films have a dielectric constant in the range of 3.0 - 3.7<sup>(4,5)</sup>. Fluorine is the most electronegative and the least polarizable element on the periodic table. Incorporation of fluorine reduces the number of polarizable Si-OH bonds and also

causes changes in the network of silicon dioxide to a less polarizable geometry<sup>(6)</sup>. These changes result in lowering the polarizability of the  $F_xSiO_y$  film itself, thus lowering the dielectric constant.

A variety of different processes to deposit fluorinated silicon dioxide films have been investigated. Conventional plasma enhanced chemical vapor deposition (PECVD), high density PECVD and atmospheric chemical vapor deposition processes (APCVD) are some of the processes that have been extensively investigated<sup>(7-11)</sup>. Recently the concept of a plasma processing apparatus with high density plasma (HDP) at low pressure has received much attention for development technology of IMD materials with half micron patterning<sup>(12,13)</sup>. Among the HDP method, helicon wave plasma CVD are being investigated with much interest, since there have been many advantages such as producing a fully ionized plasma of an efficient high density plasma at low pressure using the radio frequency waves and expanding the plasma uniformly to large diameter<sup>(14,15)</sup>. Thus, helicon wave plasma sources coupled to a reaction chamber have been providing a new method for development technology of IMD materials.

In this paper we report further results of

the formation technology of deposited SiOF films by helicon wave plasma CVD, which can discharge at 13.56 MHz fed with SiF<sub>4</sub>-O<sub>2</sub> mixtures, obtained by changing rf power, total pressure, and SiF<sub>4</sub>/O<sub>2</sub> flow ratio. The properties of deposited SiOF films such as bonding mode, F concentration, dielectric constant, leakage current, dielectric breakdown and uniformity are investigated. From these results we had found to deposition processes of SiOF films for IMD material development.

## II. EXPERIMENTAL

The SiOF films were deposited on *p*-type Si(100) 5-inch silicon substrates with SiF<sub>4</sub> and O<sub>2</sub> gases, and the addition of Ar gas by helicon wave plasma CVD as shown in Fig. 1. The wafers were chemically cleaned by a standard cleaning procedure before being loaded into the reaction chamber, and the wafer was discharged for 1 minute at Ar ambient to eliminate any contaminants on the surface. The deposition of the SiOF

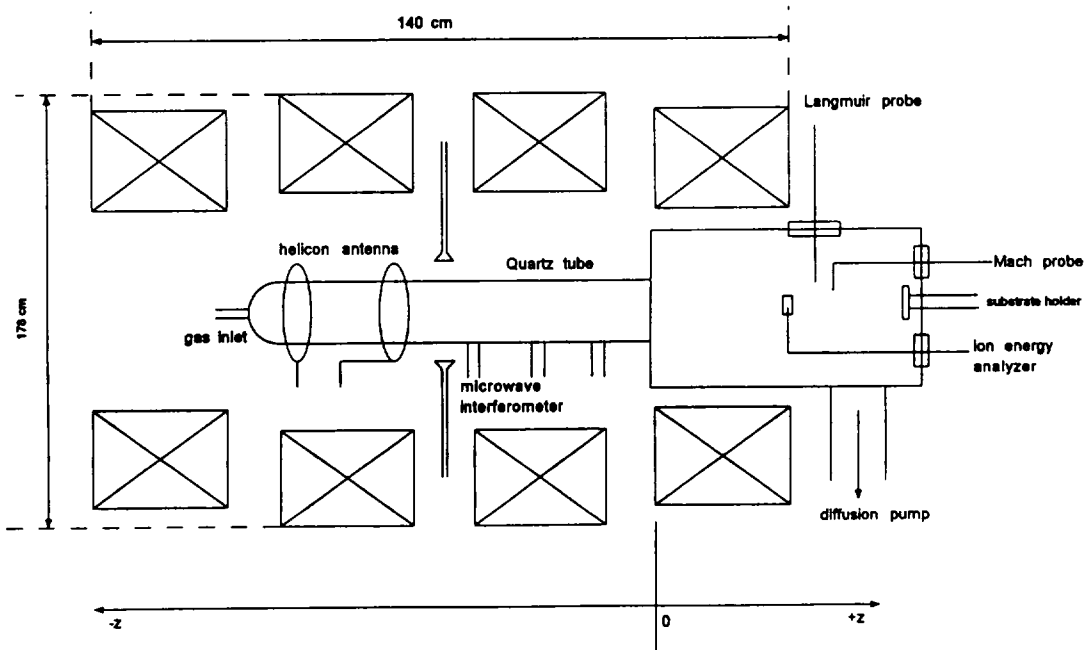


Fig. 1. The cross sectional view of the experimental apparatus for helicon wave plasma CVD system.

film is carried out as a function of the SiF<sub>4</sub>/O<sub>2</sub> flow rate ratio and rf power. Typical variable settings of the deposition process are

an rf power of 1.4kW, working pressure of 10mTorr and a magnetic field strength of 707 gauss. Table 1 shows the deposition

conditions of SiOF films. The details of the HDP by Helicon wave plasma CVD system in the formation of SiOF films have been described in recent publication and will not be presented here. The refractive index was evaluated from the average of 9 point measurements within 0.6 cm from wafer edge by using an ellipsometric system Auto EL IV (Rudolph Research). Using the refractive index, film thickness was measured by using a thickness measurement system Nano Spec/AFT Model 200 (Nanometrics). Deposition rate was calculated from the average of 9 point thickness measurements on the wafer. The concentrations of Si, O and F atoms were analyzed by X-ray photoelectron spectroscopy (XPS). Fourier transform infrared (FTIR) spectroscopy, performed in absorbance mode with a model DA8 Bomem spectrometer, is used to determine the Si-F and Si-O bonding configurations in the films. Leakage current characteristics and dielectric constant, also were investigated, using MIS (Au/2100Å thick SiOF film/p-Si) structure, having Au electrode area of  $2.5 \times 10^{-3} \text{cm}^2$ . The leakage current was measured by applying negative dc voltage to the Au electrode. The dielectric constant was calculated from the maximum capacitance evaluated from 1 MHz capacitance-voltage measurement.

Optical emission spectroscopy is used to study the relation between the relative concentrations of the radical (F, Si, and O)

species and the deposition mechanism.

Table 1. A deposition condition for the SiOF films using a helicon wave plasma CVD method

Parameter	Value	Unit
Antenna structure	coil type	
Magnetic field strength	7	Gauss
rf power	1.4	kW
Working pressure	10	mTorr
Substrate temperature	room	°C
Deposition time	1	min
Ar flow rate	2	sccm
SiF <sub>4</sub> flow rate	2~6	sccm
O <sub>2</sub> flow rate	2~6	sccm

### III. RESULTS AND DISCUSSION

The F concentration in the SiOF film is independent on the SiF<sub>4</sub>/O<sub>2</sub> flow rate ratio. Thus, it seems that the structure and optical properties of the SiOF film is affected by the plasma parameters. As shown in Figure 2, the normalized emission intensities of F (703nm), Si (728nm), and O (777nm) species by the ion saturation current density are plotted as a function of rf power. As the fraction of SiF<sub>4</sub> increases, the relative densities of F and Si species increase and the relative density of O atom slowly decreases. Therefore, the concentration of Si and F in the gas phase seems to be a limiting factor determining the

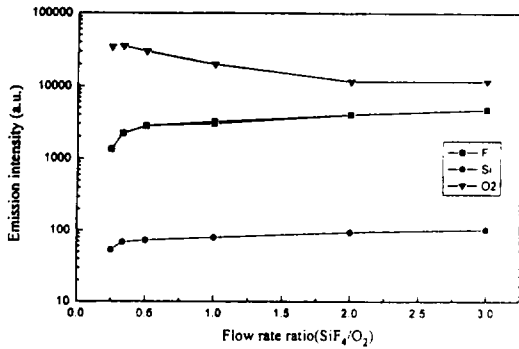


Fig. 2. The normalized emission intensities of F, Si and O as a function of the SiF<sub>4</sub>/O<sub>2</sub> flow rate ratio at B=707 Gauss and P<sub>rf</sub>=1.4 kW.

qualities of the film. The concentration of Si and F in the gas phase can be controlled by changing the flow rate ratio, operating pressure, rf power, and the magnetic field strengths. From the quantitative point of view the emission intensities of the species can be related to the concentrations of the same species in the ground state, under condition in which the decay is only radiative, through the equation

$$I \propto k_e^X n_e [X]$$

where  $k_e^X$  is the rate coefficient of the excitation process,  $n_e$  is the electron density, and  $[X]$  is the density of X species (X=F, Si, O)  $k_e^X$  is a function of the electron temperature which is nearly constant as rf power increases in the helicon plasma source. Hence, the emission intensities normalized for the ion saturation current density (or the electron density) are

representative of the relative density of each species. In the helicon mode (at high rf power of 1000W), SiF<sub>4</sub> is easily dissociated into Si, F. In the mixture of SiF<sub>4</sub> and O<sub>2</sub> gases, the threshold rf power for helicon mode is higher than that in Ar discharge. Since the helicon wave plasma has hot electron tail and high density of the electron, SiF<sub>4</sub> is very efficiently dissociated.

Figure 3 gives the FTIR absorption spectra for four of the deposited SiOF films at various SiOF<sub>4</sub> flow rate in the fixed O<sub>2</sub> gas flow rate, 4sccm. The peak corresponding to OH is not observed because a gas source containing H was not used. FTIR spectra for all of the other films we have studied are similar, with the only difference being the position of the Si-O stretching mode peak. The peak position of this mode is ranged between about 1082.45 cm<sup>-1</sup> and 1089.85 cm<sup>-1</sup>, and full width at half maximum (FWHM), as shown above, was increased from 28.65 to 82.09 as the SiF<sub>4</sub> flow rate was increased. Also the peak positions of Si-F and Si-O bond are ranged between about 917.99 cm<sup>-1</sup> and 931.06 cm<sup>-1</sup> and 812.34 cm<sup>-1</sup> and 815.04 cm<sup>-1</sup>, respectively. The peak position of Si-O stretching mode was shifted to higher wave number as the SiF<sub>4</sub>/O<sub>2</sub> flow rate ratio was increased. The spectra in the Fig. 3 are plotted in the range from 700 cm<sup>-1</sup> to 1300 cm<sup>-1</sup>, where they show the two characteristic IR bands of the Si-O-Si group<sup>[16,17]</sup>.

The O atom displacements for these variations are also indicated in the diagram. In each instance, the Si atom motion is in a direction opposite to that of the oxygen atom<sup>[16,17]</sup>. The intermediate frequency and the weakest peak at about  $810\text{ cm}^{-1}$  is a bending mode in which the oxygen atom motion is in the plane of Si-O-Si bond and along the direction of the bisector of the Si-O-Si angle (approximately  $150^\circ$ ): and

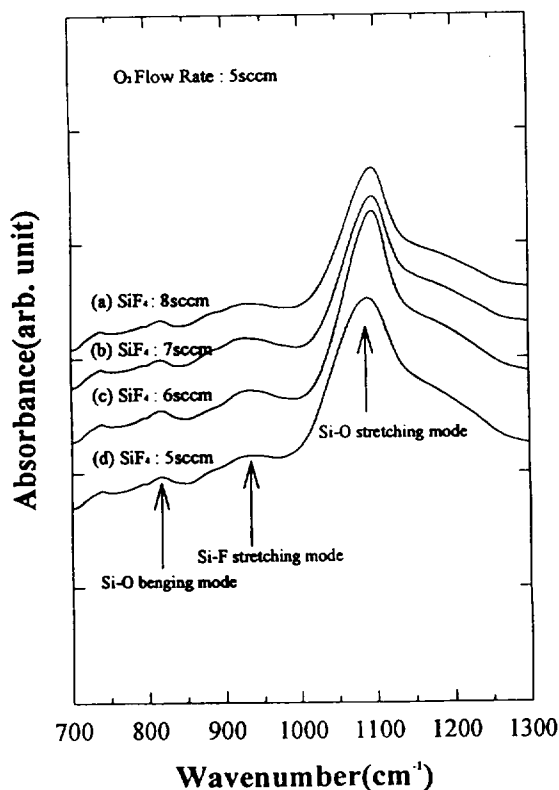


Fig. 3. FT-IR spectra of the deposited SiOF films at various  $\text{SiF}_4$  gas flow rate. (a) 8 sccm, (b) 7 sccm, (c) 6 sccm and (d) 5 sccm.

finally, the strongest peak near  $1085\text{ cm}^{-1}$  is stretching mode in which the oxygen atom motion is in the plane of the Si-O-Si bond and in a direction parallel to a line joining the two silicon atoms.

Figure 4 and 5 show the spectra of fitted data in the Fig.3. The spectra is corresponded to the imaginary part of dielectric constant by the relation of the equation that  $A \propto \nu \epsilon_r'$ , where A is the absorbance,  $\nu$  is the peak position, and  $\epsilon_r'$  is the dielectric constant. A Gaussian is corresponded to Si-O-Si bending mode and Si-F stretching mode. The peak positions of Si-O-Si stretching mode were abruptly increased by the addition of F and appeared at about  $1084.44\text{ cm}^{-1}$ .

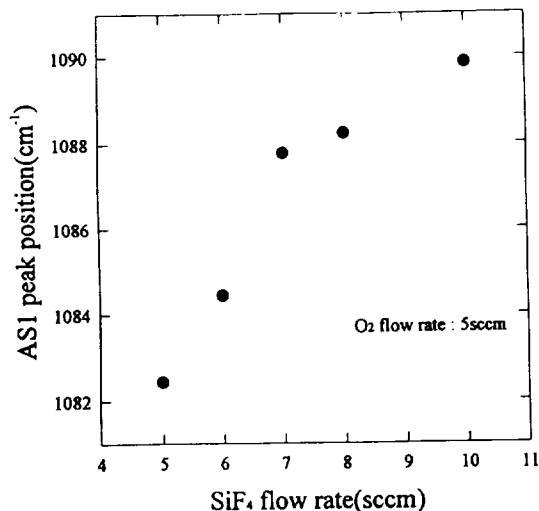


Fig. 4. The ASI peak position obtained from the IR spectra as a function of the  $\text{SiF}_4$  flow rate.

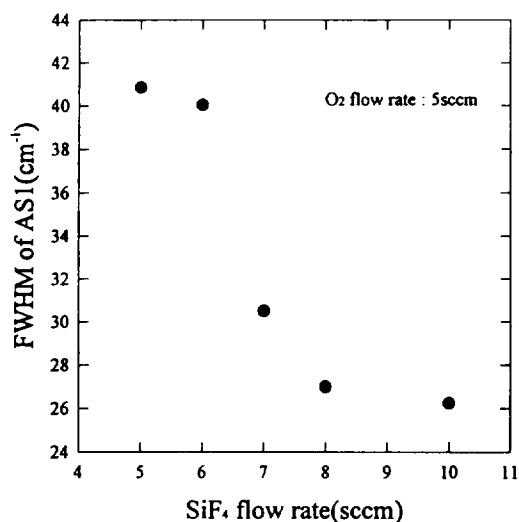


Fig. 5. The FWHM of AS1 peak obtained from the IR spectra as a function of the SiF<sub>4</sub> flow rate.

This peak position is at higher wave number than that of thermal oxides (about 1060 cm<sup>-1</sup>). On the other hand, the FWHM of AS1 mode which was decreased due to the increase of SiF<sub>4</sub> flow rate is about 40.86 cm<sup>-1</sup> (see Fig. 5). In general, it has been reported that the FWHM of LTO and TEOS-oxide are 90 cm<sup>-1</sup> and 86 cm<sup>-1</sup>, respectively, and that of thermal oxides is 71 cm<sup>-1</sup> in the thickness of 1400 Å<sup>(18)</sup>. Since the FWHM increases with thickness increasing, it can be asserted that the FWHM of AS1 mode of SiOF film is not greater than that of thermal oxides. As the difference between the FWHM's of SiOF and the thermal oxide of another authors is about 50 cm<sup>-1</sup>, we can say that the remarkable change occurs

in the FWHM of the AS1 mode, as if the thickness effect is considered. Therefore, the FWHM of SiOF is similar to thermal oxides, too.

From these experimental results, we suggest the "bond-termination" effect of F atom in the SiO<sub>2</sub> films. As the films are being grown, F atoms are bonded to Si atom with breaking of Si-O-Si chains and the arms of F-bonded Si in the surface are terminated. The arm is relatively free and rarely interact with the neighboring atoms. Therefore, the residual Si-O bondings are positioned in equilibrium angles and the bond angles are less dispersed. The after-grown films are to be "relatively" regular and the films grown finally are similar to thermal oxides.

The evolution of the refractive index in the SiOF film are shown in Fig. 6 as a function of the SiF<sub>4</sub> flow rate. As the SiF<sub>4</sub> flow rate increases, the refractive index decreases from 1.5 to 1.372. From the results in Fig. 5, the wave number of Si-O stretching mode are decreased as the refractive index increases. Because the systematic decreases in the vibrational frequency, as well as the accompanying increases in the index of refraction, derive from the replacement of Si-O bonds with Si-Si bonds as the deposition is changed from SiO<sub>2</sub> to SiOF. The change in the vibrational frequency is driven jointly by these changes in the local bonding within

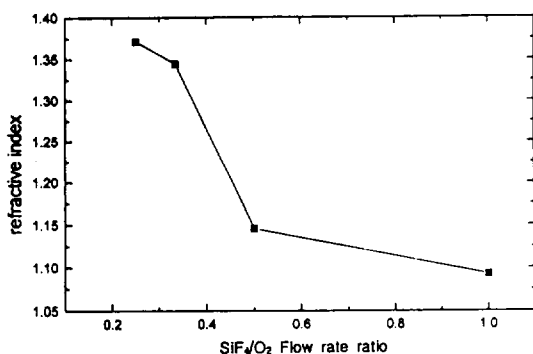


Fig. 6. The Refractive index dependence on the SiF<sub>4</sub>/O<sub>2</sub> gas flow rate ratio.

the tetrahedra and by accompanying decreases in the short range interatom force constants<sup>(19)</sup>. This last value is lower than the refractive index of a thermally grown oxide. Generally, it is known that the film of low refractive index has low dielectric constant; i.e., the increases in the index of refraction in suboxide films can be understood quantitatively in terms of the Lorentz-Lorentz<sup>(20)</sup> formalism where two factors contribute: (i) decreases in the molar volume as the Si content increases; and (ii) differences between the polarizations of Si-O, Si-F and Si-Si bonds. The Lorentz-Lorentz relationship is given by

$$\frac{(e-1)}{(e+2)} = \frac{4\pi}{3} \frac{N}{V_m} \sum f_j \alpha_j$$

where  $e=n^2$  is the optical frequency dielectric constant,  $N$  is Avogadro's number,  $V_m$  is the molar volume, and the sum is taken over the polarizabilities  $\alpha_j$  of Si-O,

Si-F and Si-Si bonds, and  $f_j$  is the fraction of each bond type.

Figure 7 shows a typical C-V characteristic of MIS (Au/SiOF/p-Si) capacitor, which the film deposited at flow rate of SiF<sub>4</sub>/O<sub>2</sub> = 5sccm/5sccm without buffer gas. As shown in this figure, the maximum

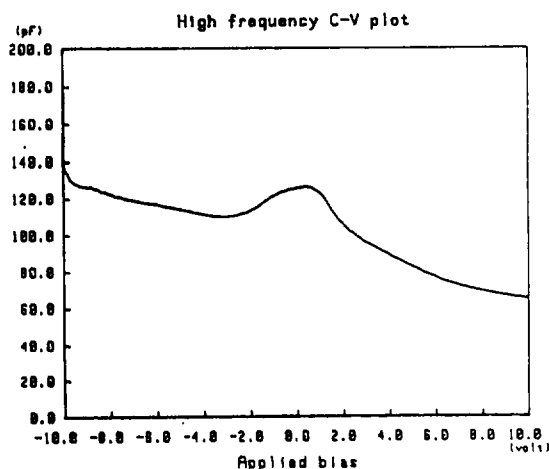


Fig. 7. C-V plot of MIS (Au/2500Å thick SiOF film/p-Si) capacitor of which the SiOF films deposited at the flow rate of SiF<sub>4</sub> : O<sub>2</sub> = 5 sccm : 5 sccm.

capacitance is measured 9.0 pF, therefore, the dielectric constant of this film was evaluated from the  $C = \epsilon_0 \epsilon_r d/A$  relation is about 3.0. The dielectric constant of deposited film at flow rate of SiF<sub>4</sub>/O<sub>2</sub> = 5sccm/4sccm without buffer gas is obtained about 3.27 (see Fig. 8, the maximum capacitance is measured 2.34 pF). Also the dielectric constant of deposited film at flow rate of SiF<sub>4</sub>/O<sub>2</sub> = 6sccm/5sccm without



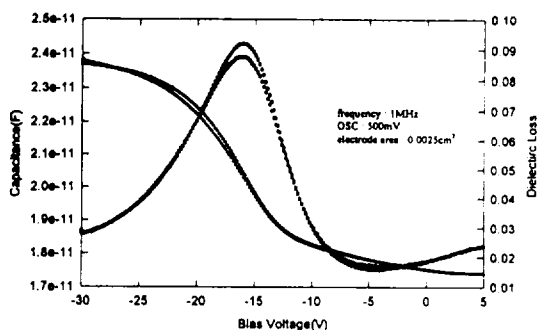


Fig. 8. C-V plot of MIS(Au/3100Å thick SiOF film/p-Si) capacitor of which the SiOF films deposited at the flow rate of SiF<sub>4</sub> : O<sub>2</sub> = 5 sccm : 4 sccm.

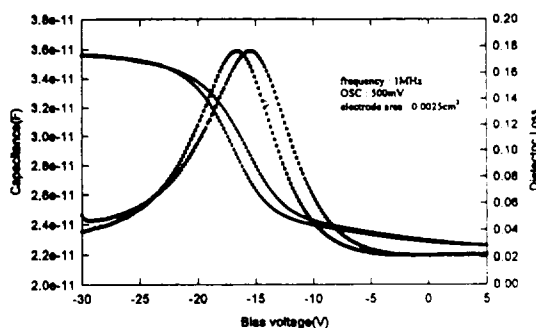


Fig. 9. C-V plot of MIS(Au/2100Å thick SiOF film/p-Si) capacitor of which the SiOF films deposited at the flow rate of SiF<sub>4</sub> : O<sub>2</sub> = 6 sccm : 5 sccm.

buffer gas is obtained about 3.38 (see Fig. 9, the maximum capacitance is measured 3.57 pF). But we have obtained that the dielectric constant of SiOF films decreases from 4.3 to 3.0 as SiF<sub>4</sub>/O<sub>2</sub> flow rate ratio increases from 0.2 to 1.0. We know that the dielectric constant of the SiOF film was affected by SiF<sub>4</sub> flow rate within the range of SiF<sub>4</sub>/O<sub>2</sub> = 1 flow rate ratio. This smaller dielectric constant is due to the fluorine atom contained in the film and to less residual OH radical, and is consistent with the smaller value of the refractive index. The low dielectric constant of SiOF films depends on the polarizability of F atom, which is given as the following equation.

$$\epsilon_{rj} = 1 + x_{rj}(\epsilon_0) = 1 + \frac{\sum N_j \alpha_j}{1 - \frac{4\pi}{3} \sum \alpha_j}$$

where  $\epsilon_{rj}$  is the dielectric constant of the SiOF film,  $x_{rj}$  is the dipole moment,  $N_j$  is the atomic concentration of the SiOF film,  $\alpha_j$  is taken over the polarizability of the  $j$  atom.

Figure 10, 11 and 12 show a typical I-V characteristic of MIS(Au/SiOF/p-Si) capacitor in the Fig. 7, 8 and 9. The applied voltage for I-V measurements are from 0 volt to 100 volt. the dielectric breakdown is the dc voltage at which permanent dielectric breakdown occurred and then the one is divided by film thickness. As shown in the Fig. 10, the leakage current suddenly increased at 13 volt. It shown that the breakdown behaviour of the SiOF film is appeared at 13 volt, and leakage current density was measured  $2.6 \times 10^{-11}$  A/cm<sup>2</sup>. Figure 11 is not observed breakdown voltage within 100V, and the dielectric break-

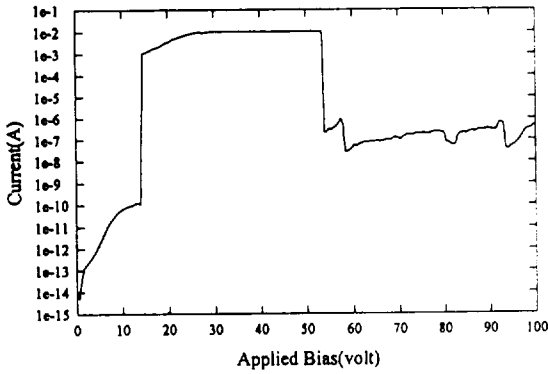


Fig. 10. I-V characteristics of MIS capacitor for the investigation of leakage current and dielectric breakdown in the Fig. 7 sample.

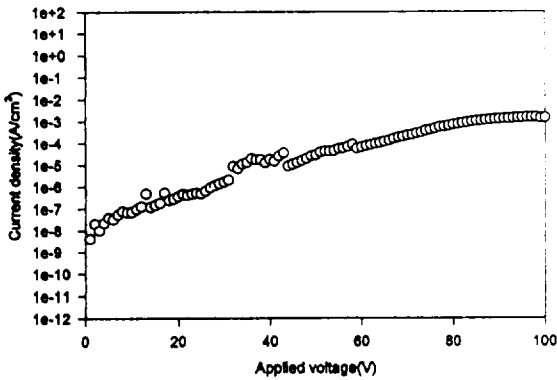


Fig. 11. I-V characteristics of MIS capacitor for the investigation of leakage current and dielectric breakdown in the Fig. 8 sample.

down and leakage current are  $>3$  MV/cm and in the range of  $4 \times 10^{-9}$  A/cm<sup>2</sup>, respectively. The dielectric breakdown and leakage current density in the Fig. 12 are

similar in the Fig. 11. These results indicate that the formed SiOF films by helicon wave plasma CVD have the excellent electrical properties and is effective for higher device operating speed.

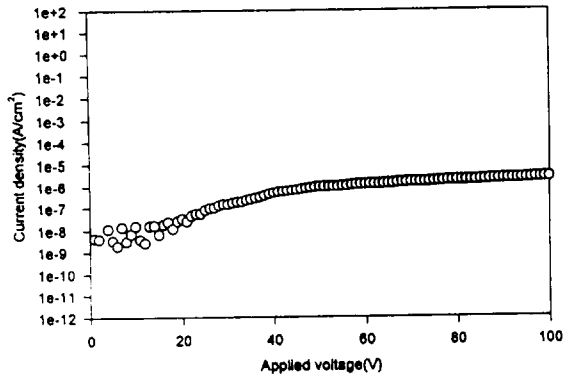


Fig. 12. I-V characteristics of MIS capacitor for the investigation of leakage current and dielectric breakdown in the Fig. 9 sample.

#### IV. CONCLUSION

A new dielectric film formation technology by helicon wave plasma CVD method has been developed. A high density plasma of  $> 10^{12}$  cm<sup>-3</sup> can be obtained by using helicon wave plasma source. The SiOF film deposition is performed on (100), p-type 5-inch silicon substrates with SiF<sub>4</sub> and O<sub>2</sub> gases, and the addition of Ar has without heating the substrate. Si-O stretching mode is observed at 1090 cm<sup>-1</sup> in the spectra of SiOF film deposited at SiF<sub>4</sub> : O<sub>2</sub> = 5sccm :

5sccm but OH radical is not observed. The SiOF films are denser than thermal oxide films. The dependence of refractive index on SiF<sub>4</sub>/O<sub>2</sub> flow rate ratio decreases from 1.37 to 1.08 as flow rate ratio increases from 0.2 to 1.0. This value is lower than that of thermal oxide and depends on F concentration. The obtained relative dielectric constant, leakage current and dielectric breakdown are about 3.0,  $<10^{-9}$  A/cm<sup>2</sup> and  $>12$  MV/cm, respectively. This technology has capability for interlayer formation in future ULSI multilevel interconnections.

## REFERENCES

- [1] J. R. Wiesner, Solid State Tech. 63, (1993).
- [2] T. Homma, Y. Kutsuzawa, K. Kum-inune, and Y. Murao, Thin Solid Films, 235, 80(1993).
- [3] M. Matsuura, Y. Hayashide, H. Kotani, and H. Abe, Jpn. J. Appl. Phys. 30, 1530(1995).
- [4] T. Fakuda, T. Akahori, First International Dielectrics for Multilevel Interconnection Conference Proceedings, DUMIC, 43(1995).
- [5] T. Matsuda, M. J. Shapiro, and S. V. Nguyen, First International Dielectrics for Multilevel Interconnection Conference Proceedings, DUMIC, 22 (1995).
- [6] N. Hakaysaka, et al., Dry Process Symposium Proceedings, 163(1993)
- [7] Y. Ikeda, Y. Numasawa, and M. Sakamoto, J. Electro. Mat., 19, 45 (1990)
- [8] M. Matsuura, Y. Hayashide, H. Kotani, and H. Abe, Jpn. J. Appl. Phys. 30, 1530(1991)
- [9] H. Kotani, M. Matsuura, A. Fuji, H. Genjon, and S. Nagao, IEEE Intern. Electron Devices Meeting, 669(1989)
- [10] M. Hatanaka, Y. Mizushima, O. Hataishi, and Y. Furumura, International IEEE VLSI Multilevel Interconnection Conference, 435(1991)
- [11] C. S. Pai, J. F. Miner, and P. D. Foo, *ibid.*, 442(1991)
- [12] D. A. Perry and R. W. Boswell, Appl. Phys. Lett. 55, 148(1989)
- [13] N. Jiwari, et al., J. Vac. Sci. Technol., A12, 1322(1994)
- [14] D. P. Lymberopoulos and D. J. Economon, J. Vac. Sci. Technol. A12, 1229, (1994)
- [15] J. M. cook et al., J. Vac. Sci. Technol. A4, 1820(1990)
- [16] F. L. Galeener, Phys. Rev. B19, 4292 (1979); F. L. Galeener and P. N. Sen, *ibid.* 17, 1928(1979)
- [17] P. N. Sen and M. F. Thorpe, Phys. Rev. B15, 4030(1977)
- [18] P. Lange, U. Schnakenberg, S. Ullerich; and H. J. Schliwinski, J. Appl. Phys. 68, 3532(1990)

- [19] G. Lucovsky, M. J. Manitini, J. K. Srivastava, and E. A. Irene, *J. Vac. Sci. Technol.* B5, 530(1987)
- [20] J. E. Stonworth, *Physical Properties of Glass*, 56(Clarendon, Oxford, 1950)